Development 125, 4669-4679 (1998)
Printed in Great Britain © The Company of Biologists Limited 1998
DEV4028

Strain-dependent embryonic lethality in mice lacking the retinoblastoma-related p130 gene

Jennifer E. LeCouter, Boris Kablar, Peter F. M. Whyte, Chuyan Ying and Michael A. Rudnicki*

Institute for Molecular Biology and Biotechnology, McMaster University, 1280 Main Street West, Hamilton, Ontario, Canada L8S 4K1
*Author for correspondence (e-mail: rudnicki@mcmaster.ca)

Accepted 21 September; published on WWW 9 November 1998

SUMMARY

The retinoblastoma-related p130 protein is a member of a conserved family, consisting of Rb, p107 and p130, which are believed to play important roles in cell-cycle control and cellular differentiation. We have generated a null mutation in *p130* by gene targeting and crossed the null allele into Balb/cJ and C57BL/6J strains of mice. In an enriched Balb/cJ genetic background, *p130*$^{-/-}$ embryos displayed arrested growth and died between embryonic days 11 and 13. Histological analysis revealed varying degrees of disorganization in neural and dermamyotomal structures. Immunohistochemistry with antibody reactive with Islet-1 indicated markedly reduced numbers of neurons in the spinal cord and dorsal root ganglia. Immunohistochemistry with antibody reactive with desmin indicated a similar reduction in the number of differentiated myocytes in the myotome. The myocardium of mutant embryos was abnormally thin and resembled an earlier staged two-chambered heart consisting of the bulbus cordis and the ventricular chamber. TUNEL analysis indicated the presence of extensive apoptosis in various tissues including the neural tube, the brain, the dermomyotome, but not the heart. Immunohistochemistry with antibody reactive with PCNA revealed increased cellular proliferation in the neural tube and the brain, and decreased proliferation in the heart. The placentas of *p130*$^{-/-}$ embryos did not display elevated apoptosis and were indistinguishable from wild type suggesting that the phenotype was not due to placental failure. Following a single cross with the C57BL/6 mice, *p130*$^{-/-}$ animals were derived that were viable and fertile. These results indicate that *p130* in a Balb/cJ genetic background plays an essential role that is required for normal development. Moreover, our experiments establish that second-site modifier genes exist that have an epistatic relationship with *p130*.

Key words: p130, Balb/C, Embryonic lethality, Mouse, Retinoblastoma

INTRODUCTION

In the developing embryo, combinatorial signals elicit appropriate patterning and morphogenesis via regulatory networks that control stem-cell determination, proliferation, differentiation and programmed death (Slack, 1992). The retinoblastoma (Rb) family, including *Rb*, *p107* and *p130*, plays an integral role in these regulatory pathways, in part by negatively regulating E2F-dependent transcription (Weinberg, 1995). Moreover, an important role for p130 in repressing cell cycle progression during differentiation is supported by the observation that p130:E2F complexes are predominant in differentiated cells (Muller, 1995; Nevins et al., 1997). Different members of the Rb-family also regulate the activity of other transcription factors including the developmentally important paired homeodomain-containing proteins MHox, Chx10 and Pax-3 (Wiggan et al., 1997), as well as the transcriptional control proteins C/EBP and c-Myc (Chen et al., 1996; Weinberg, 1995; Whyte, 1995).

Rb-family members differentially bind cyclins and their associated kinases (cyclin-dependent kinases or Cdks) resulting in the differential phosphorylation of Rb-members during progression through the cell cycle. Consequently, Rb, p107 and p130 are hypophosphorylated during different phases of the cell cycle allowing the formation of complexes that contain different E2F transcription factors (Nevins et al., 1997). The multimember E2F-family of transcription factors regulates the transcription of many genes, for example, thymidylate synthase, ribonucleotide reductase M2, DHFR, B-myb and cdc2 that are involved in DNA synthesis and cell-cycle progression. Complexes containing hypophosphorylated Rb-family members are believed to bind promoters at E2F sites and inhibit transcription by recruiting HDAC1, a histone deacetylase, to repress gene expression via chromatin remodeling (Brehm et al., 1998; Luo et al., 1998; Magnaghi-Jaulin et al., 1998). Presumably, the cyclic activation and repression of E2F-regulated genes facilitates appropriate gene expression and hence progression through the cell cycle (Muller, 1995).

Mice carrying targeted mutations in *Rb* display phenotypes supportive of a role for Rb in cellular differentiation. Homozygous mutant embryos die in utero between day 13.5 and day 15.5 of gestation and exhibit defects in erythropoiesis and extensive cell death in the central nervous system (Clarke

et al., 1992; Jacks et al., 1992; Lee et al., 1992, 1994; Macleod et al., 1996). Chimeras containing both wild-type and Rb-deficient cells are viable, but exhibit adrenal medulla hyperplasias, pituitary tumors and lens cataracts (Maandag et al., 1994; Williams et al., 1994). Unlike *Rb*-deficient embryos, $Rb^{-/-}$:wild-type chimeras contain mature *Rb*-deficient erythrocytes suggesting that erythroid differentiation is delayed rather than blocked in the absence of Rb.

Mice lacking either *p107* or *p130* in a mixed 129/Sv:C57BL/6J genetic background exhibit no overt phenotype, are viable and fertile, and embryonic fibroblasts derived from the mutants display normal cell-cycle kinetics (Cobrinik et al., 1996; Herrera et al., 1996; Hurford et al., 1997; Lee et al., 1996). Embryos lacking both *Rb* and *p107* die in utero 2 days earlier than *Rb*-deficient embryos and exhibit apoptosis in the liver and central nervous system suggesting some redundancy in function. Compound mutant mice lacking both *p130* and *p107* die soon after birth and exhibit defective endochondral bone development likely due to a deficiency in osteoblast differentiation. Taken together, these data suggested that p107 and p130 have relatively subtle roles in regulating the cell cycle and that a significant degree of overlap in function exists between the proteins (Cobrinik et al., 1996; Lee et al., 1996).

We have independently derived a targeted null mutation in *p130* into the germline of mice. In our experiments, we bred chimeras with mice from the Balb/cJ strain. Surprisingly, we observed that mice lacking *p130* displayed an embryonic lethal phenotype associated with reduced cellular differentiation and increased apoptosis. These data strongly support the assertion that *p130* in a Balb/cJ genetic background plays an essential role that is required for normal development. Moreover, the observed strain-dependence of the phenotype suggests that second-site modifier genes exist that have an epistatic relationship with *p130*.

MATERIALS AND METHODS

Generation of p130 mutant mice

A 13 kb fragment of the *p130* locus was cloned from a J1 genomic library and was used to construct a targeting vector containing 3 kb of 5′- and 7.2 kb of 3′-homologous sequence. The PGK-neo expression cassette was inserted in the opposite transcriptional orientation to p130 immediately downstream of the codon encoding aa 106 (Fig. 1). The *p130* targeting vector was linearized with *Not*I and gene targeting performed with the J1 line of ES cells as described previously (Rudnicki et al., 1992). Targeting events were detected by Southern analysis of *Eco*RV-digested genomic DNA using a 5′ flanking probe. Two independent targeted lines were injected into Balb/cJ blastocyst stage embryos to generate chimeras. Chimeras were subsequently mated to Balb/cJ females and the resulting heterozygous mice were bred to produce homozygous mutant mice. Care of animals was in accordance with institutional guidelines.

Northern and immunoblot analysis

Northern analysis of total RNA (10 μg) was performed using standard techniques with the full-length mouse *p130* cDNA as probe (LeCouter et al., 1996). Immunoblot analysis was performed as follows. Protein lysates were prepared by lysing in modified TNE (1 mM NaV and 10 μg/ml PMSF, aprotinin, pepstatin and leupeptin) or EBC lysis buffer (50 mM Tris HCl, pH 7.5, 0.5% NP40, 150 mM NaCl and protease inhibitors). Protein (30 μg) was electrophoresed on 7.5% SDS-polyacrylamide gels and transferred to PVDF membranes. Membranes blocked with 5% skim milk powder in TBST were incubated for 1 hour at room temperature with anti-p130 antibody C-20 (Santa Cruz) diluted 1:500. Following five washes in TBST, secondary antibody (diluted 1:2000) was incubated at RT for 1 hour. After five TBST washes, proteins were visualized by ECL detection (Amersham).

Histopathology and immunohistochemistry

Preparation, fixation, sectioning and staining of tissue samples for light microscopy of histological preparations were performed as described previously (Kablar et al., 1997). Following timed matings, embryos were isolated at different stages of gestation and fixed in 4% paraformaldehyde in PBS for 12-20 hours. Processing and staining with antibodies reactive with Isl-1 (Developmental Hybridoma Bank), desmin (Dako) and PCNA (Dakopatts) was performed as previously described (Kablar et al., 1997). TUNEL analysis was performed with the ApopTag Kit (Oncor). All sections were lightly counterstained with hematoxylin.

RESULTS

Targeted inactivation of *p130* in mice

The *p130* gene was disrupted by homologous recombination in J1 embryonic stem (ES) cells using standard techniques (Rudnicki et al., 1992). The *p130* targeting vector was constructed by inserting the PGK-neo cassette (McBurney et al., 1991) into a 1 kb deletion originating from a *Bam*HI site introduced into an exon immediately downstream of the codon encoding aa 160 to a *Kpn*I site within the downstream intron. The PGK-neo cassette was inserted in the opposite transcriptional orientation to *p130* (Fig. 1A). Approximately 1% of G418-resistant clones contained the targeted *p130* allele as revealed by Southern analysis. A probe upstream of the targeting vector detected an 18.5 kb *Eco*RV fragment from the wild-type *p130* allele, whereas an 7.5 kb *Eco*RV fragment was detected following homologous recombination (Fig. 1B).

Chimeras were generated following microinjection of two independently derived targeted ES lines into Balb/cJ blastocysts. Southern analysis of tail DNA in $p130^{+/-}$ germline progeny revealed the predicted restriction fragment length polymorphism (not shown). Two independent *p130* mutant mouse lines were derived into the germline and the observed homozygous embryonic lethal phenotype was completely identical in all experiments and are hereafter discussed together (see below).

To confirm that the engineered disruption of *p130* by PGK-neo had generated a null mutation, we examined expression of p130 at the level of mRNA and protein by northern and immunoblot analysis. RNA and protein was isolated from E14 embryos from an enriched C57BL/6 genetic background as previously described (LeCouter et al., 1998). Northern analysis was performed on total RNA using the full-length mouse *p130* cDNA as probe (Fig. 1C). The mature 4.9 kb *p130* mRNA was readily detected in wild-type total RNA (Fig. 1C, lane 1) and the level of *p130* mRNA was reduced by about half in $p130^{+/-}$ total RNA (Fig. 1C, lane 2). However, no *p130* mRNA was detected in RNA isolated from $p130^{-/-}$ samples (Fig. 1C, lane 3).

Immunoblot analysis was performed with antiserum C20 (Santa Cruz) reactive with the carboxyl-terminal 20 aa of p130. The p130 protein was readily detected in wild-type extracts and

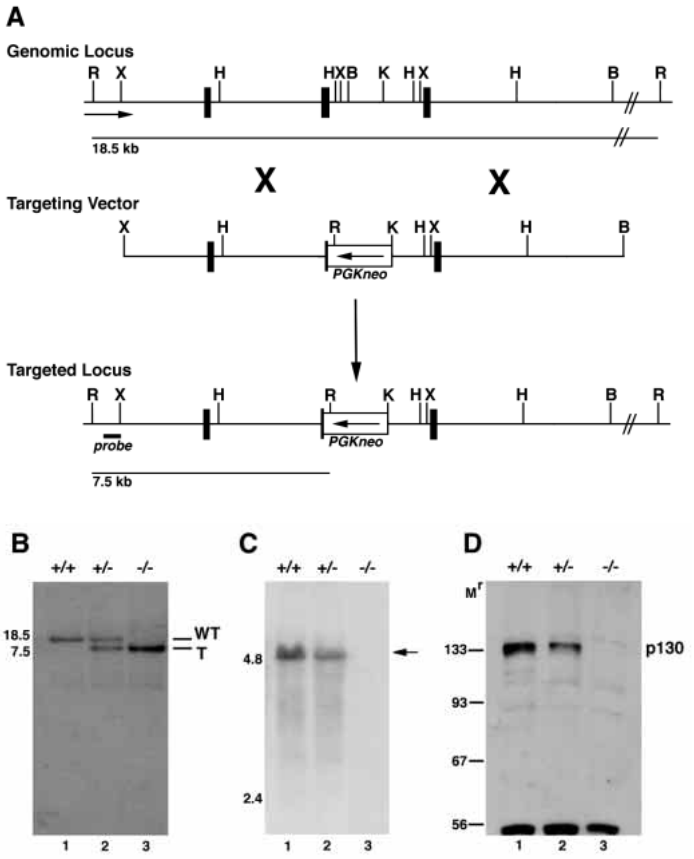

Fig. 1. Targeted disruption of the *p130* gene. (A) Genomic locus, targeting vector and structure of the disrupted *p130* locus with exons depicted as filled boxes. The targeting vector contained 3 kb of 5′- and 7.2 kb of 3′-homologous sequence. The PGK-neo expression cassette was inserted in the opposite transcriptional orientation to *p130* immediately downstream of the aa 106 codon. (B) Southern analysis of *Eco*RV-digested DNA isolated from E11.5 embryos derived from a heterozygous intercross resulted in the predicted restriction length polymorphism. (C) Northern blot analysis of total RNA probed with the full-length mouse cDNA revealed a complete absence of a transcript from the targeted *p130* allele. (D) Immunoblot analysis with antibody C20 reactive with p130 (Santa Cruz) against tissue lysates indicated that no protein was expressed from the targeted allele. Abbreviations: E, *Eco*RV; X, *Xba*I; H, *Hin*dIII; B, *Bam*HI; M_r, relative mobility in kD.

reduced levels were observed in *p130*$^{+/-}$ extracts (Fig. 1D, lanes 1 and 2). No detectable product was detected in *p130*$^{-/-}$ lysates (Fig. 1D, lane 3). Moreover, no smaller molecular weight species were apparent in *p130*$^{-/-}$ extracts. Therefore we conclude that disruption of p130 with PGK-neo generated a null allele.

Embryonic lethality in the absence of *p130*

Genotyping of the weaned 3-week-old progeny derived from interbreeding of *p130*$^{+/-}$ mice revealed an absence of *p130*$^{-/-}$ animals. Moreover, inspection of newly delivered litters revealed no increased incidence of non-viable newborn pups. Together, this suggested that *p130*$^{-/-}$ embryos were not being delivered and indicated that *p130*$^{-/-}$ embryos were dying in utero.

Table 1. Viability of embryos derived from *p130*$^{+/-}$ interbreeding

	Days post coitum					
Genotype	9.5	10.5	11.5	12.5	13.5	14.5
Wild type	6	17	15	13	9	5
p130$^{+/-}$	15	31	23	23	13	14
p130$^{-/-}$	4	14	9	2	0	0

The F_1 *p130*$^{+/-}$ offspring of chimeras bred with Balb/cJ mice were interbred and Cesarean sections performed at different gestational ages. Note, the morning following mating is considered 0.5 days post coitum.

To delineate the gestational stage that *p130*$^{-/-}$ embryos were being lost, Cesarean sections were performed at successive days postcoitum (dpc) following timed matings (Table 1). DNA was isolated from the fetal portion of the placenta and the conceptuses genotyped by Southern analysis. At 9.5 dpc and 10.5 dpc, we observed an approximate Mendelian frequency of 1:2:1 of wild-type, *p130*$^{+/-}$ and *p130*$^{-/-}$ genotypes. However, about 50% of the expected numbers of *p130*$^{-/-}$ embryos were observed on 11.5 dpc, whereas only about 10% of the expected numbers of *p130*$^{-/-}$ embryos were observed on 12.5 dpc. On and after 13.5 dpc, no viable *p130*$^{-/-}$ embryos were detected (Table 1). In addition, we observed that approximately 25% of the conceptuses were non-viable and were undergoing absorption on and after 12.5 dpc. Therefore, we conclude that a null mutation in *p130* in a Balb/cJ genetic background resulted in an embryonic lethal phenotype with embryos dying between embryonic day 11 and 13.

Embryos lacking *p130* display abnormal growth

Inspection of *p130*$^{-/-}$ embryos revealed a disparity in growth that increased with gestational age until 11.5 dpc when the mutant embryo reached approximately 25% of the normal size (Fig. 2A). Mutant embryos at 10.5 dpc exhibited beating hearts with seemingly normal vascularization and distribution of blood. However, mutant hearts displayed an abnormal dilated morphology and appeared to resemble the two-chambered hearts of earlier-stage embryo. More anterior structures appeared normal, for example, 10.5 dpc *p130*$^{-/-}$ embryos exhibited normal brain segmentation, normal elaboration of branchial arches and normal morphology of forelimbs. Posterior structures were reduced and mutant 10.5 dpc embryos failed to form hind limb buds. By 11.5 dpc, the remaining viable mutant embryos had progressed little in development and appeared similar in size to 10.5 dpc *p130*$^{-/-}$ embryos (Fig. 2A).

One possible explanation for the observed growth arrest of *p130*$^{-/-}$ embryos was that function of the placenta was compromised due to abnormal placental development. Importantly, dissection of the placentas from *p130*$^{-/-}$ embryos revealed a normal anatomy and arrangement of extraembryonic blood vessels and membranes. Histological analysis of hematoxylin-stained sections indicated a normal cytomorphology including that of giant cells and placental labyrinth. To assess the extent of apoptosis in *p130*$^{-/-}$ placentas, TUNEL analysis was performed to detect the presence of fragmented DNA in apoptotic bodies (Gavrieli et al., 1992). Importantly, no evidence of apoptosis was detected by TUNEL staining (Fig. 3). Taken together, these data support

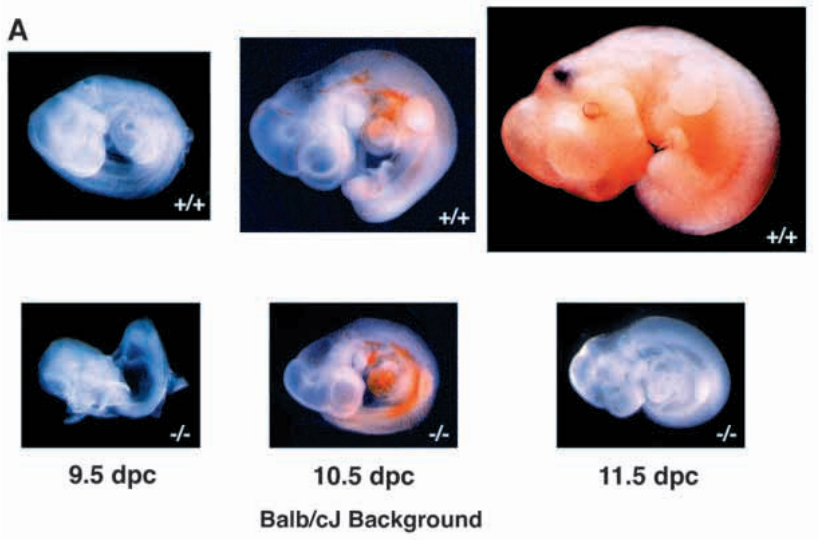

Fig. 2. Embryonic growth deficiency in the absence of p130 is strain-dependent. (A) Wild-type embryos at 9.5 dpc have turned whereas *p130*$^{-/-}$ embryos were typically observed in the lordotic position and displayed reduced numbers of somites. By 10.5 dpc, *p130*$^{-/-}$ embryos are about half the normal size of wild-type embryos and displayed normal development of brain structures, however more posterior structures, including the heart and the hind limb region, were underdeveloped. The mutant embryo at 11.5 dpc was strikingly smaller than wild type and appeared arrested at the E10.5 stage. (B) In the C57Bl/6J genetic background, *p130*$^{-/-}$ mice were viable, fertile and displayed no overt phenotype (see Table 2). Note, 9.5 dpc and 10.5 dpc embryos were photographed before fixation, whereas 11.5 dpc embryos were photographed postfixation.

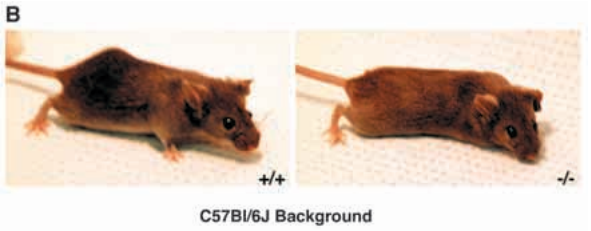

the conclusion that the growth deficit of *p130*$^{-/-}$ embryos was not due to placental failure.

Impaired neurogenesis and myogenesis in *p130*$^{-/-}$ embryos

Histological examination of sections of 10.5 dpc *p130*$^{-/-}$ embryos revealed some variability in the histological appearance of embryos presumably reflecting their overall viability. A typical 10.5 dpc *p130*$^{-/-}$ embryo that exhibited a beating heart when delivered is described below. Histological analysis revealed varying degrees of disorganization in neural and dermamyotomal structures, a poorly formed notochord and, in addition, a thin myocardium (Figs 4, 5).

Neuroepithelial cells within the neural tube are the progenitors of motor neurons that differentiate in response to signals from the floor plate of the neural tube (Yamada et al., 1991, 1993). To assess neuronal differentiation, immunohistochemistry was performed with antibody reactive against the LIM-domain transcription factors Isl-1 and Isl-2, expressed in newly born motor and sensory neurons (Ericson et al., 1992; Tsuchida et al., 1994). We observed severely decreased numbers of Isl-1/2-expressing motor neurons within the ventral horn of a somewhat disorganized neural tube and similarly decreased numbers of sensory neurons within a poorly demarcated dorsal root ganglia (compare Fig. 4A and B). Moreover, the neural epithelium in the neural tube entirely failed to elaborate a basement membrane and cells were not organized into layers as in the wild-type neural tube (Figs 4B,D, 5). The floorplate of the neural tube was observed to have undergone marked apoptotic loss at thoracic and lumbar levels (compare Figs 4A and B, 5A and B). However, reduced numbers of neurons were noted at all levels.

The somite-derived dermamyotome, segmentally arranged on either side of the neural tube, forms the first differentiated skeletal muscle of the embryo known as the myotome (Hauschka, 1994). Myogenic differentiation was assessed with antisera reactive to desmin, an intermediate filament protein expressed in skeletal and cardiac muscle (Kablar et al., 1997). The differentiated myotome of wild-type embryos at 10.5 dpc displayed the typical pattern of desmin-expressing myocytes (Fig. 4C). By contrast, the differentiated myotome of *p130*-deficient embryos was composed of very few desmin-expressing skeletal myocytes (compare Fig. 4C and D). The observed reduction in numbers of myotomal myocytes was also found at all levels.

Inspection of 10.5 dpc *p130*$^{-/-}$ embryos revealed a somewhat dilated myocardium and abnormal cardiac morphology suggestive of a defect in chamber formation (Fig. 2A). To characterize cardiac structure of *p130*$^{-/-}$ embryos, serial sections were performed through the hearts and

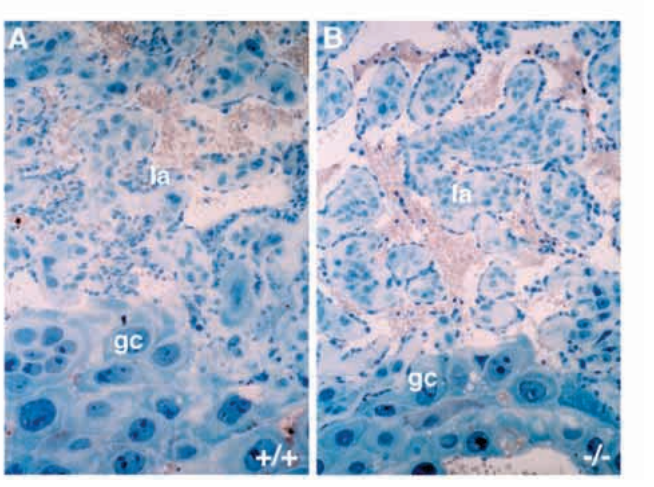

Fig. 3. Normal placental cytomorphology and absence of apoptosis of p130-deficient placentas. The placentas of wild-type (A) and *p130*$^{-/-}$ (B) embryos were identical in appearance and both contained very few apoptotic bodies. Abbreviations: gc, giant cells; la, labyrinth. Panels were photographed at a magnification of 400×.

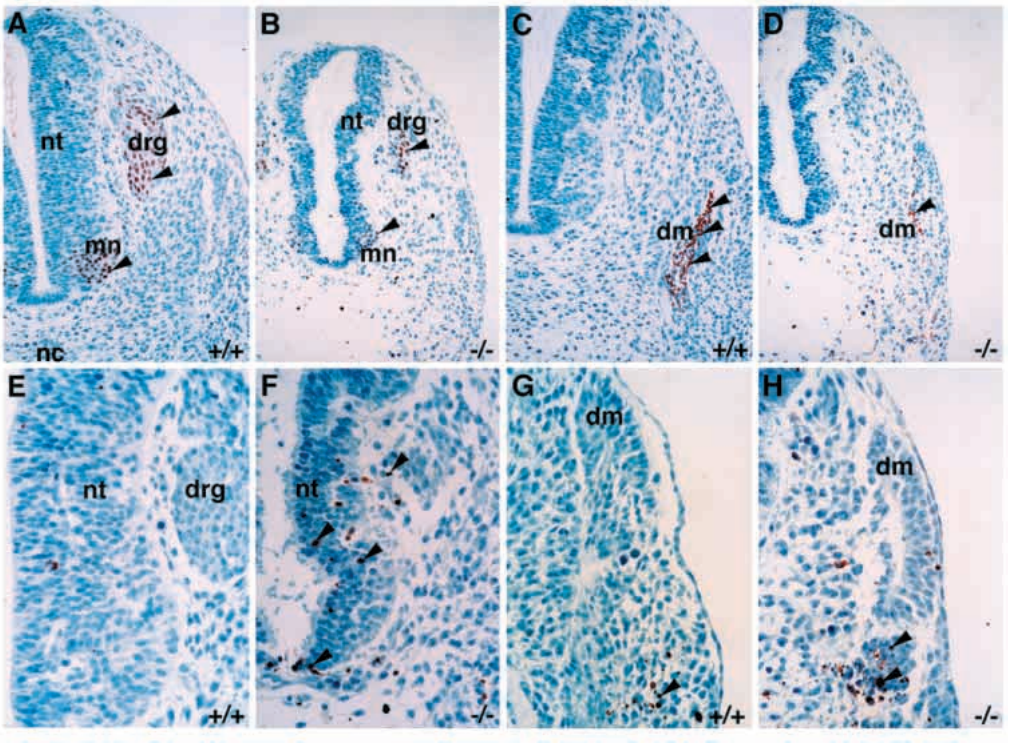

Fig. 4. Deficient myogenesis and neurogenesis and associated apoptosis in E10.5 *p130*$^{-/-}$ embryos. Wild-type embryos (A) contained numerous motor and sensory neurons in the neural tube and dorsal root ganglia as detected with antibody reactive to Isl-1/2. Embryos lacking p130 (B) were reduced in size, displayed a disorganized morphology and contained severely reduced numbers of Isl-1/2-expressing motor and sensory neurons. The normal myotome of wild-type embryos (C) was reduced to a small rudiment in *p130*$^{-/-}$ embryos (D) as revealed by staining with antibody reactive to desmin. TUNEL analysis revealed low levels of apoptosis in wild-type embryos (E,G) and markedly increased numbers of apoptotic bodies (arrowheads) in the neural tube, dorsal root ganglia and dermamyotome of *p130*$^{-/-}$ embryos (F,H). Note the absence of the notochord, the disorganized neural floor plate and absence of a basement membrane in the neural tubes of *p130*$^{-/-}$ embryos (B,F). Abbreviations: nt, neural tube; nc, notochord; mn, motor neurons; drg, dorsal root ganglia; dm, dermamyotome. Panels were photographed at magnification of 200× (A-D), 400× (E-H).

immunohistochemistry was performed with antibody reactive with desmin. The myocardium of *p130*$^{-/-}$ embryos was poorly developed with a thin wall usually only a single cell in thickness. However, the pericardium and endocardium appeared normal. Examination of serial sections revealed a failure to properly loop and form the four-chambered heart (compare Fig. 6A and B, C and D). Instead, the mutant heart somewhat resembled the two chambered E8.5 heart consisting of the bulbus cordis and the ventricular chamber (Fig. 6).

Increased apoptosis and cellular proliferation in *p130*$^{-/-}$ embryos

The observed deficiency in neurogenic and myogenic development and presence of numerous subcellular bodies suggested that many cells in *p130*$^{-/-}$ embryos had undergone programmed death. Therefore, to assess the levels of apoptosis in *p130*-deficient embryos, we performed TUNEL analysis on sectioned material. Wild-type embryos typically contained few apoptotic cells disseminated through the neural tube and dermamyotome (Figs 4E,G, 5A). By contrast, *p130*$^{-/-}$ embryos contained numerous apoptotic bodies throughout the neural tube and floor plate, and within the epithelial and delaminating portions of the dermamyotome (Figs 4F,H, 5B). In addition, extensive apoptosis was also observed in the midgut and urogenital ridge, but not the mesonephros (Fig. 6). Moreover, little or no apoptosis was detected in the *p130*$^{-/-}$ lung bud,

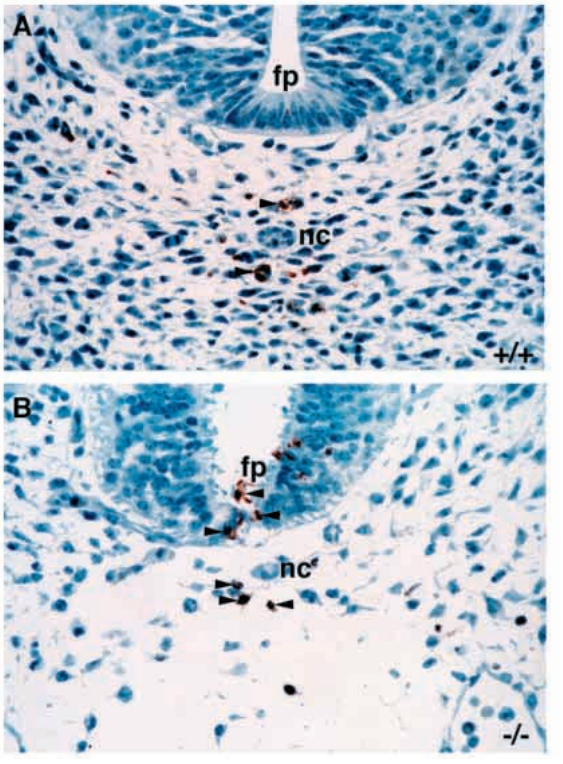

Fig. 5. Loss of floor plate in E10.5 *p130*$^{-/-}$ embryos. TUNEL analysis revealed low levels of apoptosis in wild-type neural tube (A) and markedly increased numbers of apoptotic bodies (arrowheads) in the neural tube of *p130*$^{-/-}$ embryos (B). Note the almost complete absence of a floor plate in the *p130*$^{-/-}$ neural tube. Abbreviations: fp, floor plate; nc, notochord. Panels were photographed at magnification of 400×.

foregut and hepatic primordia (Fig. 7). Note that the morphological development of the midgut, urogenital ridge, mesonephros, lung bud, foregut and liver primordia were at an appropriate stage for 10.5 dpc embryos but appeared abnormal due to markedly reduced cellularity in surrounding structures and poorly elaborated basement membranes. Interestingly, the myocardium of *p130*$^{-/-}$ embryos, like the wild-type myocardium, contained very few apoptotic nuclei (Fig. 8E,F). Taken together, these data suggest that the absence of *p130* differentially affects the differentiation or survival of myotomal and neuronal cells versus cardiac myocytes.

Examination of neural structures in the heads of *p130*$^{-/-}$ embryos suggested that cell survival within the developing central nervous system was severely perturbed in the absence of *p130*. TUNEL analysis of 10.5 dpc *p130*$^{-/-}$ embryos revealed reduced size and extensive apoptosis in the optic vesicle (Fig. 9E), optic stalk (Fig. 9G), facial acoustic neural crest complex (Fig. 9I) and otic vesicle (Fig. 9K). By contrast, wild-type embryos displayed only moderate numbers of apoptotic bodies in head neural structures (Fig. 9A,D,F,H,J). Interestingly, *Rb*-deficient embryos display elevated apoptosis and inappropriate proliferation in brain and retinal neurons (Clarke et al., 1992; Jacks et al., 1992; Lee et al., 1992, 1994; Maandag et al., 1994). Therefore, taken together these data suggest that Rb and p130 play important functions in coupling cellular differentiation to cell-cycle control, particularly in the context of neural cell development.

To investigate whether *p130*$^{-/-}$ embryos exhibited inappropriate proliferation, we performed immunohistochemistry with antibody PC10 reactive with proliferating cell nuclear antigen (PCNA). Replicating cells

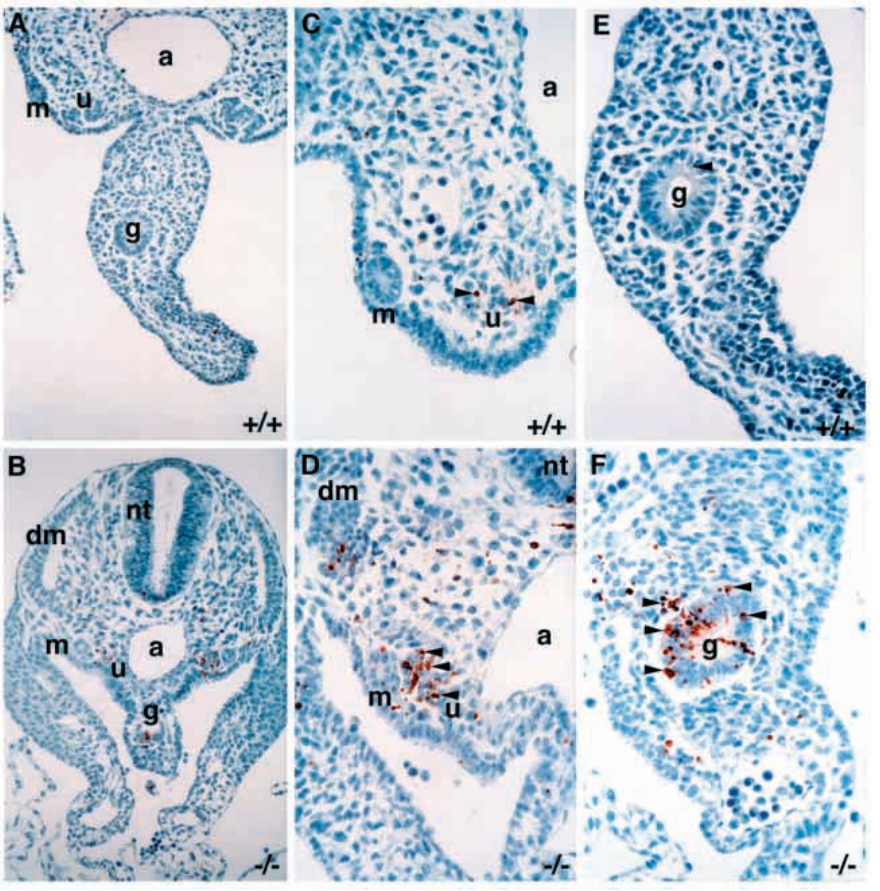

Fig. 6. Increased apoptosis in the urogenital ridge and midgut in *p130*$^{-/-}$ 10.5 dpc embryos. TUNEL analysis revealed low levels of apoptosis in wild-type embryos (A,C,E) and markedly increased numbers of apoptotic bodies (arrowheads) in the urogenital ridge (B,D) and midgut (B,F) of *p130*$^{-/-}$ embryos. Abbreviations: a, midline dorsal aorta; dm, dermamyotome; g, midgut; m, mesonephric duct/vesicle; nt, neural tube; u, urogenitol ridge. Panels were photographed at magnification of 200× (A-D) and 400× (C-F).

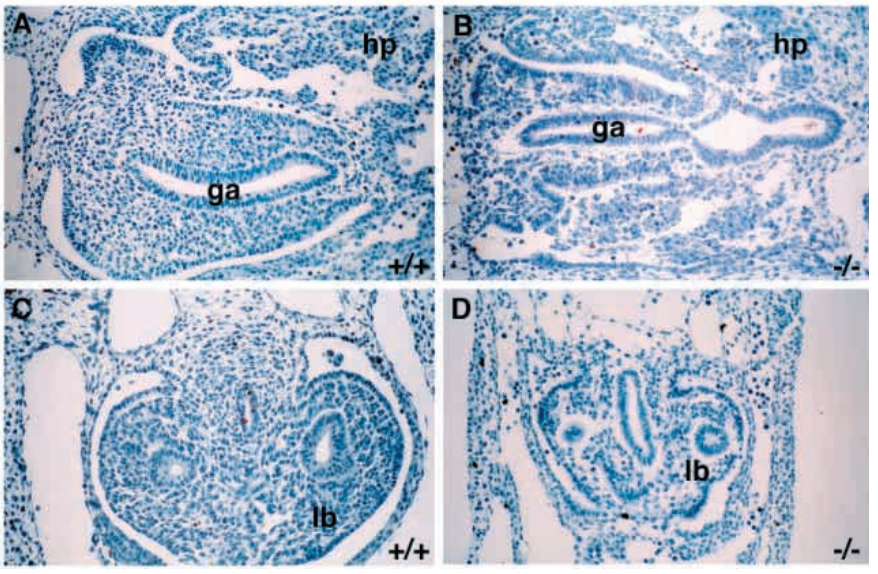

Fig. 7. Absence of apoptosis in lung bud, foregut and hepatic primordia in E10.5 *p130*$^{-/-}$ embryos. TUNEL analysis revealed negligible levels of apoptosis in both wild-type (A,C) and *p130*$^{-/-}$ (B,D) lung bud, foregut and hepatic primordia. Abbreviations: lb, lung bud; ga, gastric dilatation of foregut; hp, hepatic/bilary primordia. Panels were photographed at magnification of 400×.

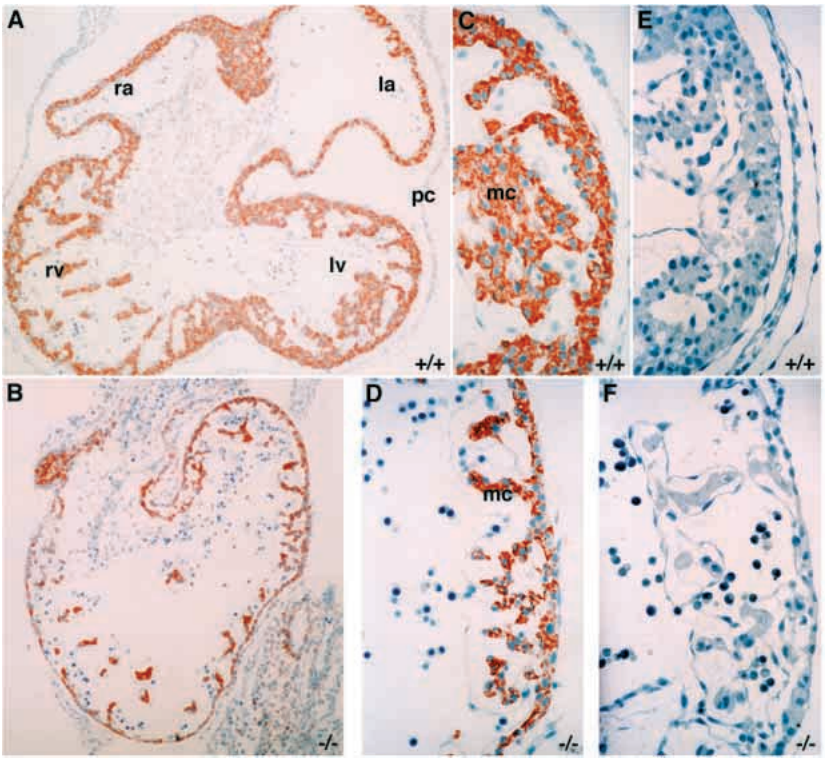

Fig. 8. Abnormal cardiogenesis in *p130*$^{-/-}$ embryos. Immunochemistry with antibody reactive with desmin revealed the four-chambered myocardium of wild-type embryos (A,C). By contrast, the myocardium of *p130*$^{-/-}$ embryos (B,D) was poorly developed and serial sections indicated the presence of two-chambers, the bulbus cordis and the ventricular chamber. TUNEL analysis did not reveal any significant apoptosis in wild-type (E) or mutant (F) hearts. Abbreviations: m, myocardium; pc, pericardium; ra, right atria; la, left atria; rv, right ventricle; lv, left ventricle. Panels were photographed at magnification of 100× (A,D) and 400× (B,C,E,F).

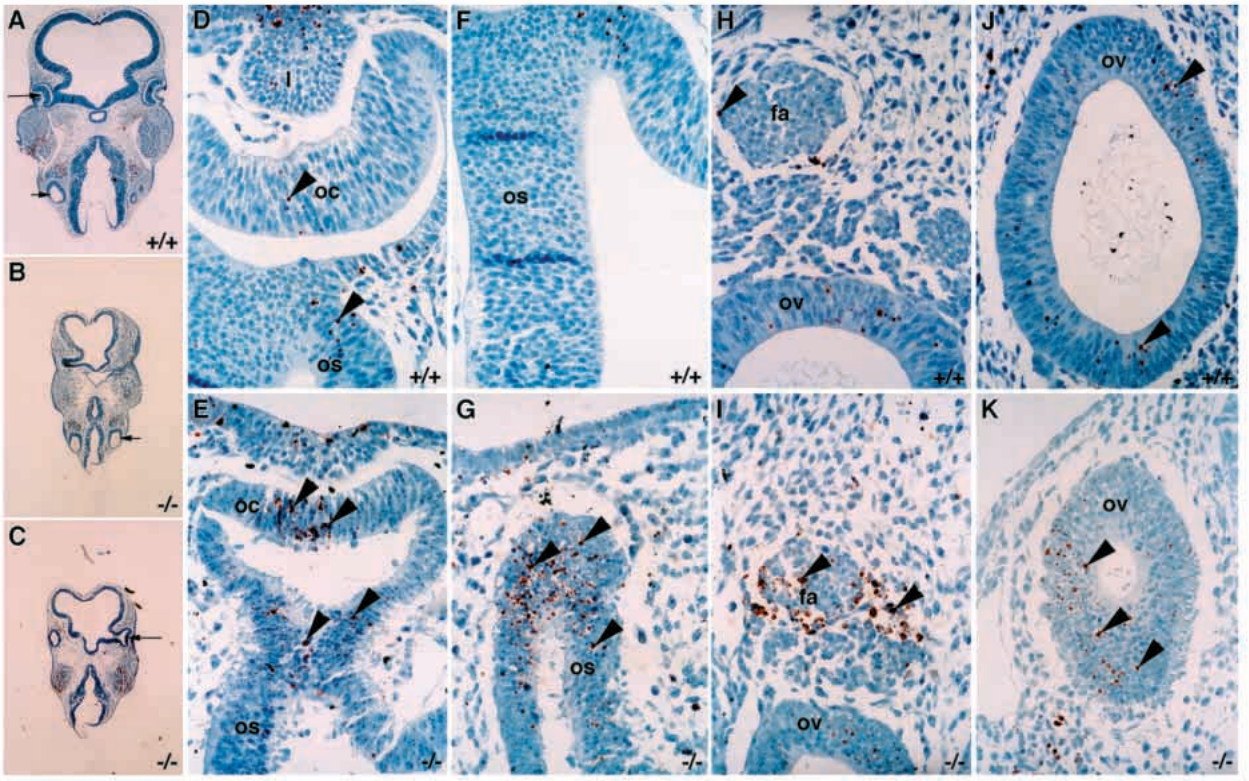

Fig. 9. Increased apoptosis and poor differentiation of head neural structures in the absence of p130. TUNEL analysis of 10.5 dpc wild-type embryos (A) revealed moderate numbers of apoptotic bodies in the optic vesicles (D), optic stalks (F), facial acoustic neural crest complexes (H) and otic vesicles (J). The head neural structures of *p130*$^{-/-}$ embryos (B, C) displayed reduced size and extensive apoptosis in the optic vesicles (E), optic stalks (G), facial acoustic neural crest complexes (I) and otic vesicles (K). Note the absence of a basement membrane lining the neural structures of *p130*$^{-/-}$ embryos. In A-C, long arrow denotes optic vesicle and stalk, and short arrow denotes otic vesicle. In the remainder of the panels, arrowheadss indicate TUNEL-positive cells. Abbreviations: oc, optic cup; os, optic stalk; fa, facio-auditory pre-ganglion complex; ov, otic vesicle. Panels were photographed at 400× magnification with the exception of A-C, at 25×.

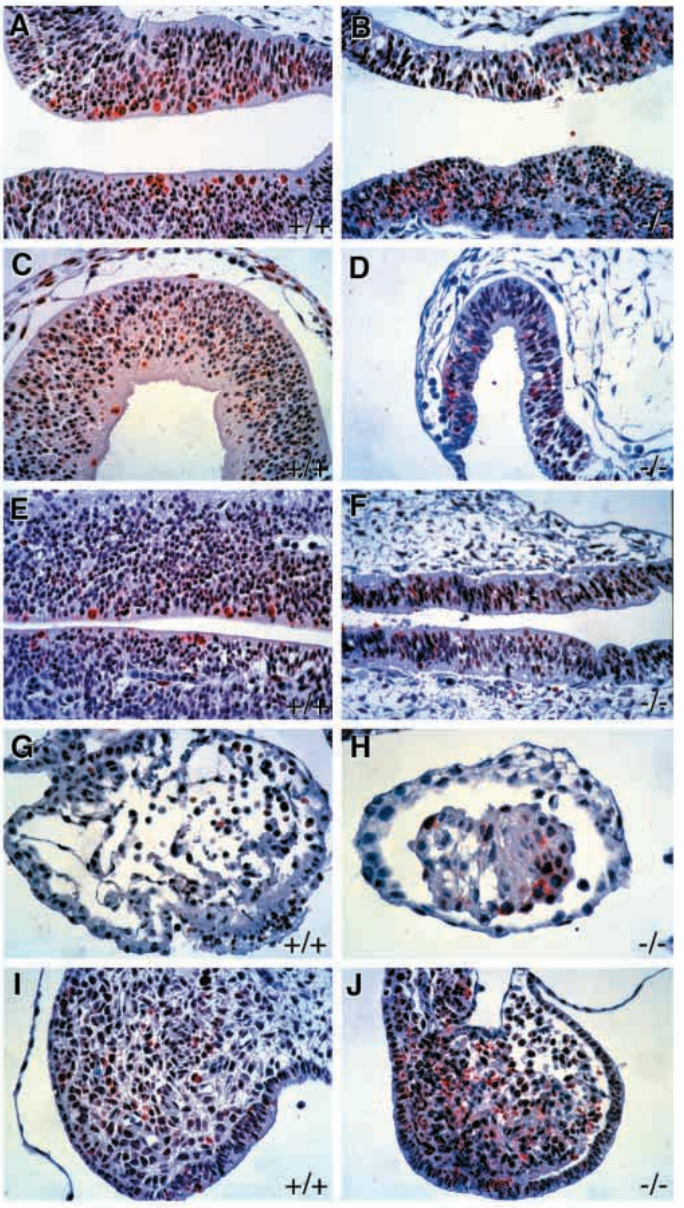

Fig. 10. Detection of increased cellular proliferation by PCNA-expression. Immunohistochemistry of sectioned E10.5 *p130*$^{-/-}$ embryos with antibody PC10 revealed over a 2-fold increase in numbers of PCNA-expressing cells as revealed by nuclear staining in the telencephalon (A,B), diencephalon (C,D) and the neural tube (E,F). By contrast, *p130*$^{-/-}$ cardiac muscle contained 1.6-fold fewer proliferative cells (G,H) and no difference in the proportion of PCNA-expressing cells was observed between mutant and wild-type branchial arches (I,J). Panels were photographed at 400× magnification.

express PCNA at high levels during S-phase thus immunodetection of PCNA in tissues allows a determination of relative mitotic activity (Megeney et al., 1996). In 10.5 dpc *p130*$^{-/-}$ embryos, the numbers of PCNA-expressing cells were increased 2.1-fold in the telencephalon (Fig. 10A,B), 2.6-fold in the diencephalon (Fig. 10C,D) and 2.1-fold in the neural tube (Fig. 10E,F). By contrast *p130*$^{-/-}$ cardiac muscle contained 1.6-fold fewer PCNA-expressing cells (Fig. 10G,H), and no difference in the proportion of PCNA-expressing cells was observed between mutant and wild-type branchial arches (Fig. 10I,J). Therefore, a tissue-specific correlation between the presence of inappropriate proliferation and increased apoptosis was evident in *p130*$^{-/-}$ embryos.

Table 2. Genetic background specifies the penetrance of the *p130*$^{-/-}$ phenotype

	Intercross		
	Chimera × Balb/cJ ↓	$F_1^{+/-}$ × Balb/cJ ↓	$F_1^{+/-}$ × C57BL/6J ↓
Genotype	$F_1^{+/-} \times F_1^{+/-}$*	$B_1^{+/-} \times B_1^{+/-}$‡	$B_1^{+/-} \times B_1^{+/-}$§
Wild type	42	12	21
p130$^{+/-}$	78	28	39
p130$^{-/-}$	0	0	24

*The F_1 *p130*$^{+/-}$ progeny of the founding chimeras bred with Balb/cJ mice when interbred yielded no viable *p130*$^{-/-}$ pups.

‡The B_1 *p130*$^{+/-}$ mice derived from an F_1 *p130*$^{+/-}$ × Balb/cJ mating when interbred also failed to produce *p130*$^{-/-}$ mice.

§The B_1 *p130*$^{+/-}$ mice, derived from a F_1 *p130*$^{+/-}$ × C57BL/6J mating, when interbred generated litters that contained viable and fertile *p130*$^{-/-}$ mice that displayed an apparently normal phenotype (see Fig. 2B).

The *p130* mutant phenotype is strain dependent

The relatively normal phenotype of the *p130*$^{-/-}$ mice previously described in a mixed 129/Sv:C57BL/6J genetic background (Cobrinik et al., 1996) and the embryonic lethal phenotype of *p130*$^{-/-}$ mice in an enriched Balb/cJ background suggested that the penetrance of the *p130*$^{-/-}$ phenotype was dependent on second site modifier genes. To test this hypothesis, we bred F_1 *p130*$^{+/-}$ mice, the progeny of the founding chimeras and Balb/cJ mice, with either C57BL/6J or Balb/cJ mice. The resulting B_1 *p130*$^{+/-}$ mice were then interbred to generate *p130*$^{-/-}$ mice. The B_1 *p130*$^{+/-}$ mice derived from the F_1 *p130*$^{+/-}$ × C57BL/6J cross have one set of C57BL/6J chromosomes and a second set composed of a mixture of Balb/cJ and 129/Sv chromosomes. The 129/Sv chromosomes are derived from the embryonic stem cells. The B_1 *p130*$^{+/-}$ mice derived from the F_1 *p130*$^{+/-}$ × Balb/cJ cross have one set of Balb/cJ chromosomes and a second set composed of an undefined mixture of Balb/cJ and 129/Sv chromosomes. Thus, such crosses allow an assessment of the contribution of Balb/cJ and C57BL/6J genetic backgrounds to the penetrance of the phenotype. However, these experiments do not directly assess the contribution of the 129/Sv genetic background to the penetrance of the phenotype.

As described above, *p130*$^{-/-}$ animals derived from an F_1 *p130*$^{+/-}$ × F_1 *p130*$^{+/-}$ mating displayed 100% penetrance of the lethal phenotype (see Table 2, 1st column). In a small proportion of F_2 *p130*$^{-/-}$ × F_2 *p130*$^{-/-}$ matings, we observed litters that contained a mixture of runted and normal-sized F_3 *p130*$^{-/-}$ mice suggesting that multiple recessive second-site modifier genes were segregating in the population. Interbreeding of B_1 *p130*$^{+/-}$ mice derived from a F_1 *p130*$^{+/-}$ × Balb/cJ mating gave rise to *p130*$^{-/-}$ mice that also exhibited a 100% penetrance of the phenotype (Table 2, 2nd column). By contrast, interbreeding of B_1 *p130*$^{+/-}$ mice derived from a F_1 *p130*$^{+/-}$ × C57BL/6J mating gave rise to *p130*$^{-/-}$ mice that were viable and fertile, and displayed no detectable phenotype (Fig. 2B). Taken together, these data suggest that the C57BL/6J genetic background suppressed the *p130*$^{-/-}$ embryonic lethal phenotype apparent on a Balb/cJ genetic background (Table 2,

3rd column). Therefore, we conclude that multiple second-site modifier genes exist that have an epistatic relationship with p130.

DISCUSSION

We have generated a null allele of *p130* by gene targeting in mice and crossed the mutant allele into Balb/cJ and C57BL/6J strains of mice. Embryos lacking *p130* in a genetic background enriched for Balb/cJ were reduced in size and died between embryonic stages E11 and E13. Immunohistochemistry with Isl-1 antibody revealed profoundly reduced numbers of motor neurons in the spinal cord and sensory neurons in the dorsal root ganglia. In addition, immunohistochemistry with antibody reactive to desmin similarly indicated markedly reduced numbers of differentiated myocytes within the myotome. The hearts of mutant embryos displayed unusually thin walls and appeared delayed in development. TUNEL analysis indicated the presence of numerous apoptotic bodies in many tissues including the neural tube, dermamyotome and brain, but not in the heart or the histologically normal placenta. Immunohistochemistry with antibody reactive with PCNA revealed increased cellular proliferation in the neural tube and the brain, and decreased proliferation in the heart. Importantly, following a backcross to C57BL/6J mice, *p130*$^{-/-}$ animals were derived that were phenotypically normal. These data clearly indicate that p130 plays an essential role in development, but in a strain-dependent manner.

Embryos deficient for p130 contained low numbers of Isl-1, expressing neurons in the neural tube and low numbers of desmin-expressing myocytes in the dermamyotome. This deficiency was correlated with the presence of reduced notochord and floor plate structures in the trunk, together with increased levels of apoptosis. Several contributing mechanisms can be proposed to functionally explain the embryonic lethal phenotype in the absence of p130 in a genetic background enriched for Balb/cJ. For example, patterning and morphogenesis may be perturbed following loss of key structures during development and cellular differentiation. Alternatively, cell survival may be detrimentally affected because of a unique function of p130 in withdrawal from the cell cycle or in enforcing terminal differentiation.

Apoptotic loss of structures like the notochord during the development of *p130*$^{-/-}$ embryos could contribute significantly to the embryonic phenotype. For example, the determination of progenitors of motor neurons is regulated in part by signals from the notochord and floor plate of the neural tube (Yamada et al., 1991, 1993). Sonic hedgehog (Shh) is expressed in the notochord and the floor plate in the trunk where it functions to induce the progenitors of motor neurons. These progenitors, situated in the ventricular epithelium of the ventral neural tube, are induced to migrate laterally and to differentiate and settle in a single continuous primary motor column (Tanabe et al., 1995). Additionally, Shh, expressed in the floor plate and the notochord, and Wnt family members, expressed in the dorsal neural tube, have been suggested to combinatorially activate myogenesis in the somite (Munsterberg et al., 1995). Wnts positively stimulate myogenesis in the somite whereas Shh is believed to activate Noggin expression in the dorsal somite, inhibiting the repression of myogenesis by lateral-plate-derived BMP4 (Hirsinger et al., 1997; Marcelle et al., 1997; Reshef et al., 1998). Therefore, it is interesting to speculate that loss of structures such as the floorplate in *p130*$^{-/-}$ embryos may contribute to the severity *p130*-mutant phenotype.

A loss-of-function mutation in *p130* may also result in cell-autonomous deficits in cellular differentiation. For example, the reduced neurogenesis and myogenesis observed in *p130*$^{-/-}$ embryos may reflect a global perturbation of patterning due to specific requirements for p130 in directly negatively regulating proteins with paired-like homeodomains that play key developmental roles (Wiggan et al., 1997). Alternatively, appropriate withdrawal from the cell cycle and terminal differentiation may be detrimentally affected due to an important regulatory role played by the formation of specific E2F/p130 complexes (Muller, 1995; Whyte, 1995). For example, myoblasts contain free E2F as well as E2F complexed with p107 and to a lesser degree p130, but not Rb, whereas differentiated myocytes primarily contain E2F complexed with p130, but not p107 or Rb (Corbeil et al., 1995; Shin et al., 1995). In differentiated myocytes, E2F complexes are primarily composed of E2F-4/p130 and formation of this complex has been suggested to be a necessary event in terminal differentiation (Puri et al., 1997; Shin et al., 1995). Similarly, formation of analogous E2F/p130 complexes has been observed during both neuronal and cardiomyocyte differentiation (Flink et al., 1998; Raschella et al., 1997). Therefore, the low numbers of cells expressing Isl-1 or desmin in *p130*$^{-/-}$ embryos may reflect an important and unique role for p130 in withdrawing from the cell cycle or enforcing terminal differentiation. Clearly, the presence of markedly increased numbers of PCNA-expressing cells in tissues containing increased numbers of apoptotic cells supports this later hypothesis.

In *Rb*-deficient embryos, cells continue to replicate in regions of the central and peripheral nervous system that normally contain only postmitotic cells with many of the neurons undergoing apoptosis shortly after entering an ectopic S-phase (Lee et al., 1994). Apoptosis in the nervous system of *Rb*$^{-/-}$ embryos is p53-dependent and correlates with increased levels of E2F, cyclin E and p21 (Macleod et al., 1996). In muscle, lack of Rb similarly results in apoptotic loss of inappropriately proliferating cells that fail to undergo terminal differentiation (Wang et al., 1997; Zacksenhaus et al., 1996). Heterozygous *Rb* mice develop lens cataracts due to loss-of-homozygosity in *Rb*, in which cells are poorly differentiated, are highly proliferative and undergo very high rates of apoptosis. By contrast, heterozygous Rb mice bred into a p53-homozygous mutant background exhibit overt lens hyperplasias with no associated apoptosis (Morgenbesser et al., 1994). Similarly, transgenic mice expressing human papilloma virus type 16 (HPV-16) E7 in retinal cells exhibit very high rates of retinal cell apoptosis. However, expression of both E7 and E6 transgenes, or the E7 transgene in p53-mutant mice induces retinal tumors with a reduction or absence of associated apoptosis (Howes et al., 1994; Pan and Griep, 1994). HPV-16 E7-protein binds all Rb-family members suggesting that the failure of retinoblastomas to form in targeted Rb-mutant mice is a consequence of functional redundancy amongst the Rb-family.

Inappropriate activation of E2F in a wide variety of cell types leads to p53-enhanced apoptosis (Hiebert et al., 1995;

Phillips et al., 1997; Qin et al., 1994; Shan and Lee, 1994). Moreover, Rb and p130 appear to induce G_1 arrest via biochemically distinct mechanisms involving either E2F-1 or E2F-4 (Vairo et al., 1995). Therefore, generation of compound *p130*$^{-/-}$*:p53*$^{-/-}$ embryos in a Balb/cJ genetic background may elucidate whether the observed widespread apoptosis is p53-dependent as well as potentially allow partial rescue of the phenotype.

We have also derived a targeted null mutation in *p107* and have bred the mutant allele into either Balb/cJ or C57BL/6J genetic backgrounds. We observed that *p107*$^{-/-}$ embryos in an enriched Balb/cJ background are viable and fertile but exhibit diathetic myeloid metaplasia, a severe postnatal growth deficiency and an accelerated cell cycle (LeCouter et al., 1998). By contrast, *p107*$^{-/-}$ mice in a C57BL/6J background display no apparent phenotype (LeCouter et al., 1998; Lee et al., 1996). These data strongly support our interpretation that second-site modifier genes exist that effect the penetrance of null mutations in both *p130* and *p107*.

Mice carrying targeted null mutations (for example in *IGF-1*, *fibronectin*, *EGFR*, *CFTR*, *TGFβ1*, *TGFβ3* and *β1-adrenergic receptor*) can display highly variable penetrance of phenotype on different genetic backgrounds (Bonyadi et al., 1997; George et al., 1993; Liu et al., 1993; Proetzel et al., 1995; Rohrer et al., 1996; Rozmahel et al., 1996; Sibilia and Wagner, 1995; Threadgill et al., 1995). Clearly, these observations underscore the significance of second-site modifier genes when characterizing null mutations. The molecular basis for the penetrance of the *p130/-* phenotype on C57BL/6J versus Balb/cJ backgrounds remains to be established. Nevertheless, the breeding data is consistent with the existence of multiple modifier alleles representing either recessive loss-of-function mutations in the C57BL/6J background, dominant gain-of-function mutations in the Balb/cJ background, or a mixture of both (Table 2). Alternatively, our data does not rule out the possibility that heterozygosity at some modifier alleles contributes to the observed phenotype. In addition, our experiments do not directly assess the role played by the ES-derived 129/Sv chromosomes segregating in the different offspring. However, genetic analysis should allow a resolution of this issue. Currently, we are performing microsatellite analysis to accurately determine the number of modifying genes and to map their approximate locations. Clearly, the molecular identification of genes epistatically interacting with p130 and p107 will further our understanding of the regulatory pathways within which Rb-family members operate.

M. A. R. is a Research Scientist of the National Cancer Institute of Canada and a member of the Canadian Genetic Disease Network of Excellence. We thank Dr John Hassell for critical reading of the manuscript and Linda May for expert technical assistance. This work was supported by a grants from the National Cancer Institute of Canada to M. A. R. and P. F. M. W.

REFERENCES

Bonyadi, M., Rusholme, S. A., Cousins, F. M., Su, H. C., Biron, C. A., Farrall, M. and Akhurst, R. J. (1997). Mapping of a major genetic modifier of embryonic lethality in TGF beta 1 knockout mice. *Nat. Genet.* **15,** 207-11.

Brehm, A., Miska, E. A., McCance, D. J., Reid, J. L., Bannister, A. J. and Kouzarides, T. (1998). Retinoblastoma protein recruits histone deacetylase to repress transcription. *Nature* **391,** 597-601.

Chen, P. L., Riley, D. J., Chen-Kiang, S. and Lee, W. H. (1996). Retinoblastoma protein directly interacts with and activates the transcription factor NF-IL6. *Proc. Natl. Acad. Sci. USA* **93,** 465-9.

Clarke, A. R., Maandag, E. R., van Roon, M., van der Lugt, N. M., van der Valk, M., Hooper, M. L., Berns, A. and te Riele, H. (1992). Requirement for a functional Rb-1 gene in murine development. *Nature* **359,** 328-30.

Cobrinik, D., Lee, M. H., Hannon, G., Mulligan, G., Bronson, R. T., Dyson, N., Harlow, E., Beach, D., Weinberg, R. A. and Jacks, T. (1996). Shared role of the pRB-related p130 and p107 proteins in limb development. *Genes Dev.* **10,** 1633-44.

Corbeil, H. B., Whyte, P. and Branton, P. E. (1995). Characterization of transcription factor E2F complexes during muscle and neuronal differentiation. *Oncogene* **11,** 909-20.

Ericson, J., Thor, S., Edlund, T., Jessell, T. M. and Yamada, T. (1992). Early stages of motor neuron differentiation revealed by expression of homeobox gene Islet-1. *Science* **256,** 1555-60.

Flink, I. L., Oana, S., Maitra, N., Bahl, J. J. and Morkin, E. (1998). Changes in E2F complexes containing retinoblastoma protein family members and increased cyclin-dependent kinase inhibitor activities during terminal differentiation of cardiomyocytes. *J. Mol. Cell Cardiol.* **30,** 563-78.

Gavrieli, Y., Sherman, Y. and Ben-Sasson, S. A. (1992). Identification of programmed cell death in situ via specific labeling of nuclear DNA fragmentation. *J. Cell Biol.* **119,** 493-501.

George, E. L., Georges-Labouesse, E. N., Patel-King, R. S., Rayburn, H. and Hynes, R. O. (1993). Defects in mesoderm, neural tube and vascular development in mouse embryos lacking fibronectin. *Development* **119,** 1079-91.

Hauschka, S. D. (1994). The embryonic origin of muscle. In *Myology* (ed. A. G. Engel and C. Franzini-Armstrong), Vol. 1, pp. 3-73. New York: McGraw-Hill.

Herrera, R. E., Sah, V. P., Williams, B. O., Makela, T. P., Weinberg, R. A. and Jacks, T. (1996). Altered cell cycle kinetics, gene expression, and G1 restriction point regulation in Rb-deficient fibroblasts. *Mol. Cell Biol.* **16,** 2402-7.

Hiebert, S. W., Packham, G., Strom, D. K., Haffner, R., Oren, M., Zambetti, G. and Cleveland, J. L. (1995). E2F-1:DP-1 induces p53 and overrides survival factors to trigger apoptosis. *Mol. Cell Biol.* **15,** 6864-6874.

Hirsinger, E., Duprez, D., Jouve, C., Malapert, P., Cooke, J. and Pourquie, O. (1997). Noggin acts downstream of Wnt and Sonic Hedgehog to antagonize avian somite patterning. *Development* **124,** 4605-4614.

Howes, K. A., Ransom, N., Papermaster, D. S., Lasudry, J. G. H., Albert, D. M. and Windle, J. J. (1994). Apoptosis or retinoblastoma: alternative fates of photoreceptors expressing the HPV-16 E7 gene in the presence or absence of p53. *Genes Dev.* **8,** 1300-1310.

Hurford, R. K., Jr., Cobrinik, D., Lee, M. H. and Dyson, N. (1997). pRB and p107/p130 are required for the regulated expression of different sets of E2F responsive genes. *Genes Dev.* **11,** 1447-63.

Jacks, T., Fazeli, A., Schmitt, E. M., Bronson, R. T., Goodell, M. A. and Weinberg, R. A. (1992). Effects of an Rb mutation in the mouse. *Nature* **359,** 295-300.

Kablar, B., Krastel, K., Ying, C., Asakura, A., Tapscott, S. J. and Rudnicki, M. A. (1997). MyoD and Myf-5 differentially regulate the development of limb versus trunk skeletal muscle. *Development* **124,** 4729-38.

LeCouter, J. E., B., K., Hardy, W. R., Ying, C., Megeney, L. A., May, L. L. and Rudnicki, M. A. (1998). Strain-dependent myeloid metaplasia, growth deficiency, and shortened cell-cycle in mice lacking p107. *Mol. Cell. Biol.* (in press).

LeCouter, J. E., Whyte, P. F. and Rudnicki, M. A. (1996). Cloning and expression of the Rb-related mouse p130 mRNA. *Oncogene* **12,** 1433-40.

Lee, E. Y., Chang, C. Y., Hu, N., Wang, Y. C., Lai, C. C., Herrup, K., Lee, W. H. and Bradley, A. (1992). Mice deficient for Rb are nonviable and show defects in neurogenesis and haematopoiesis. *Nature* **359,** 288-94.

Lee, E. Y., Hu, N., Yuan, S. S., Cox, L. A., Bradley, A., Lee, W. H. and Herrup, K. (1994). Dual roles of the retinoblastoma protein in cell cycle regulation and neuron differentiation. *Genes Dev.* **8,** 2008-21.

Lee, M. H., Williams, B. O., Mulligan, G., Mukai, S., Bronson, R. T., Dyson, N., Harlow, E. and Jacks, T. (1996). Targeted disruption of p107: functional overlap between p107 and Rb. *Genes Dev.* **10,** 1621-32.

Liu, J. P., Baker, J., Perkins, A. S., Robertson, E. J. and Efstratiadis, A. (1993). Mice carrying null mutations of the genes encoding insulin-like growth factor I (Igf-1) and type 1 IGF receptor (Igf1r). *Cell* **75,** 59-72.

Luo, R. X., Postigo, A. A. and Dean, D. C. (1998). Rb interacts with histone deacetylase to repress transcription. *Cell* **92,** 463-73.

Maandag, E. C., van der Valk, M., Vlaar, M., Feltkamp, C., O'Brien, J., van Roon, M., van der Lugt, N., Berns, A. and te Riele, H. (1994). Developmental rescue of an embryonic-lethal mutation in the retinoblastoma gene in chimeric mice. *EMBO J.* **13,** 4260-8.

Macleod, K. F., Hu, Y. and Jacks, T. (1996). Loss of Rb activates both p53-dependent and independent cell death pathways in the developing mouse nervous system. *EMBO J.* **15,** 6178-88.

Magnaghi-Jaulin, L., Groisman, R., Naguibneva, I., Robin, P., Lorain, S., Le Villain, J. P., Troalen, F., Trouche, D. and Harel-Bellan, A. (1998). Retinoblastoma protein represses transcription by recruiting a histone deacetylase. *Nature* **391,** 601-5.

Marcelle, C., Stark, M. R. and Bronner-Fraser, M. (1997). Coordinate actions of BMPs, Wnts, Shh and noggin mediate patterning of the dorsal somite. *Development* **124,** 3955-3963.

McBurney, M. W., Sutherland, L. C., Adra, C. N., Leclair, B., Rudnicki, M. A. and Jardine, K. (1991). The mouse Pgk-1 gene promoter contains an upstream activator sequence. *Nucleic Acids Res.* **19,** 5755-61.

Megeney, L. A., Kablar, B., Garrett, K., Anderson, J. E. and Rudnicki, M. A. (1996). MyoD is required for myogenic stem cell function in adult skeletal muscle. *Genes Dev.* **10,** 1173-83.

Morgenbesser, S. D., Williams, B. O., Jacks, T. and DePinho, R. A. (1994). p53-dependent apoptosis produced by Rb-deficiency in the developing mouse lens. *Nature* **371,** 72-4.

Muller, R. (1995). Transcriptional regulation during the mammalian cell cycle. *Trends Genet.* **11,** 173-8.

Munsterberg, A. E., Kitajewski, J., Bumcrot, D. A., McMahon, A. P. and Lassar, A. B. (1995). Combinatorial signaling by Sonic hedgehog and Wnt family members induces myogenic bHLH gene expression in the somite. *Genes Dev.* **9,** 2911-22.

Nevins, J. R., Leone, G., DeGregori, J. and Jakoi, L. (1997). Role of the Rb/E2F pathway in cell growth control. *J. Cell Physiol.* **173,** 233-6.

Pan, H. and Griep, A. E. (1994). Altered cell cycle regulation in the lens of HPV-16 E6 or E7 transgenic mice: implications for tumor suppressor gene function in development. *Genes Dev.* **8,** 1285-1299.

Phillips, A. C., Bates, S., Ryan, K. M., Helin, K. and Vousden, K. H. (1997). Induction of DNA systhesis and apoptosis are separable functions of E2F-1. *Genes Dev.* **11,** 1853-1863.

Proetzel, G., Pawlowski, S. A., Wiles, M. V., Yin, M., Boivin, G. P., Howles, P. N., Ding, J., Ferguson, M. W. and Doetschman, T. (1995). Transforming growth factor-beta 3 is required for secondary palate fusion. *Nat. Genet.* **11,** 409-14.

Puri, P. L., Balsano, C., Burgio, V. L., Chirillo, P., Natoli, G., Ricci, L., Mattei, E., Graessmann, A. and Levrero, M. (1997). MyoD prevents cyclinA/cdk2 containing E2F complexes formation in terminally differentiated myocytes. *Oncogene* **14,** 1171-84.

Qin, X. Q., Livingston, D. M., Kaelin, W. G., Jr. and Adams, P. D. (1994). Deregulated transcription factor E2F-1 expression leads to S-phase entry and p53-mediated apoptosis. *Proc. Natl. Acad. Sci. USA* **91,** 10918-10922.

Raschella, G., Tanno, B., Bonetto, F., Amendola, R., Battista, T., De Luca, A., Giordano, A. and Paggi, M. G. (1997). Retinoblastoma-related protein pRb2/p130 and its binding to the B-myb promoter increase during human neuroblastoma differentiation. *J. Cell Biochem.* **67,** 297-303.

Reshef, R., Maroto, M. and Lassar, A. B. (1998). Regulation of dorsal somitic cell fates: BMPs and Noggin control the timing and pattern of myogenic factor expression. *Genes Dev.* **12,** 290-303.

Rohrer, D. K., Desai, K. H., Jasper, J. R., Stevens, M. E., Regula, D. P., Jr., Barsh, G. S., Bernstein, D. and Kobilka, B. K. (1996). Targeted disruption of the mouse beta1-adrenergic receptor gene: developmental and cardiovascular effects. *Proc. Natl Acad. Sci. USA* **93,** 7375-80.

Rozmahel, R., Wilschanski, M., Matin, A., Plyte, S., Oliver, M., Auerbach, W., Moore, A., Forstner, J., Durie, P., Nadeau, J., et al. (1996). Modulation of disease severity in cystic fibrosis transmembrane conductance regulator deficient mice by a secondary genetic factor. *Nat. Genet.* **12,** 280-7.

Rudnicki, M. A., Braun, T., Hinuma, S. and Jaenisch, R. (1992). Inactivation of MyoD in mice leads to up-regulation of the myogenic HLH gene Myf-5 and results in apparently normal muscle development. *Cell* **71,** 383-90.

Shan, B. and Lee, W. H. (1994). Deregulated expression of E2F-1 induces S-phase entry and leads to apoptosis. *Mol. Cell Biol.* **14,** 8166-73.

Shin, E. K., Shin, A., Paulding, C., Schaffhausen, B. and Yee, A. S. (1995). Multiple change in E2F function and regulation occur upon muscle differentiation. *Mol. Cell Biol.* **15,** 2252-62.

Sibilia, M. and Wagner, E. F. (1995). Strain-dependent epithelial defects in mice lacking the EGF receptor. *Science* **269,** 234-8.

Slack, J. M. W. (1992). Models for man: the mouse and the chick. In *From Egg to Embryo*, pp. 171-277. Cambridge: Cambridge University Press.

Tanabe, Y., Roelink, H. and Jessell, T. M. (1995). Induction of motor neurons by Sonic hedgehog is independent of floor plate differentiation. *Current Biol.* **5,** 651-8.

Threadgill, D. W., Dlugosz, A. A., Hansen, L. A., Tennenbaum, T., Lichti, U., Yee, D., LaMantia, C., Mourton, T., Herrup, K., Harris, R. C., et al. (1995). Targeted disruption of mouse EGF receptor: effect of genetic background on mutant phenotype. *Science* **269,** 230-4.

Tsuchida, T., Ensini, M., Morton, S. B., Baldassare, M., Edlund, T., Jessell, T. M. and Pfaff, S. L. (1994). Topographic organization of embryonic motor neurons defined by expression of LIM homeobox genes. *Cell* **79,** 957-970.

Vairo, G., Livingston, D. M. and Ginsberg, D. (1995). Functional interaction between E2F-4 and p130: evidence for distinct mechanisms underlying growth suppression by different retinoblastoma protein family members. *Genes Dev.* **9,** 869-81.

Wang, J., Guo, K., Wills, K. N. and Walsh, K. (1997). Rb functions to inhibit apoptosis during myocyte differentiation. *Cancer Res.* **57,** 351-4.

Weinberg, R. A. (1995). The retinoblastoma protein and cell cycle control. *Cell* **81,** 323-30.

Whyte, P. (1995). The retinoblastoma protein and its relatives. *Semin. Cancer Biol.* **6,** 83-90.

Wiggan, O., Taniguchi-Sidle, A. and Hamel, P. A. (1997). Interaction of the pRB-family proteins with factors containing paired-like homeodomains. *Oncogene* **16,** 227-236.

Williams, B. O., Schmitt, E. M., Remington, L., Bronson, R. T., Albert, D. M., Weinberg, R. A. and Jacks, T. (1994). Extensive contribution of Rb-deficient cells to adult chimeric mice with limited histopathological consequences. *EMBO J.* **13,** 4251-9.

Yamada, T., Pfaff, S. L., Edlund, T. and Jessell, T. M. (1993). Control of cell pattern in the neural tube: motor neuron induction by diffusible factors from notochord and floor plate. *Cell* **73,** 673-86.

Yamada, T., Placzek, M., Tanaka, H., Dodd, J. and Jessell, T. M. (1991). Control of cell pattern in the developing nervous system: polarizing activity of the floor plate and notochord. *Cell* **64,** 635-47.

Zacksenhaus, E., Jiang, Z., Chung, D., Marth, J. D., Phillips, R. A. and Gallie, B. L. (1996). pRb controls proliferation, differentiation, and death of skeletal muscle cells and other lineages during embryogenesis. *Genes Dev.* **10,** 3051-3064.